Bull. Mater. Sci., Vol. 35, No. 1, February 2012, pp. 19–25. © Indian Academy of Sciences.

Dielectric properties and structural dynamics of melt compounded hot-pressed poly(ethylene oxide)–organophilic montmorillonite clay nanocomposite films

R J SENGWA* **and SHOBHNA CHOUDHARY**
Department of Physics, J N V University, Jodhpur 342 005, India

MS received 9 January 2010; revised 16 June 2011

Abstract. The dielectric properties of melt compounded hot-pressed nanocomposite films consisting of a poly(ethylene oxide) (PEO) and organophilic montmorillonite (OMMT) clay surface modified with trimethyl stearyl ammonium as filler with increasing amount up to 20 wt.% OMMT were investigated in a frequency range of 20 Hz–1 MHz at 30 °C. The predominance of OMMT exfoliated structures in PEO–OMMT nanocomposites were recognized by a decrease of the real part of complex dielectric function. OMMT concentration dependent dielectric and electric modulus relaxation times have revealed that the interactions compatibility between PEO molecules and dispersed OMMT nano-platelets in PEO matrix governs the PEO segmental dynamics. A.C. conductivity of these nanocomposites increases by two orders of magnitude in the experimental frequency range.

Keywords. PEO–OMMT nanocomposites; dielectric relaxation; electrical conductivity; impedance spectroscopy.

1. Introduction

Synthesization and structural characterization of polymer–clay nanocomposite (PCN) films and colloids have been an intense topic of industrial and academic research (Tunney and Detellier 1996; Ogata *et al* 1997; Liao *et al* 2001; Shen *et al* 2002, 2003; Chaiko 2003; Strawhecker and Manias 2003; Chen and Evans 2004; Lin-Gibson *et al* 2004; Nelson and Cosgrove 2004; Homminga *et al* 2005; Reinholdt *et al* 2005; Elmahdy *et al* 2006; Hikosaka *et al* 2006; de Bruyn *et al* 2008; Liu *et al* 2008; Miwa *et al* 2008; Sengwa *et al* 2008, 2009a–c, 2010a–c; Sengwa and Choudhary 2010, 2011). These investigations on organic–inorganic nanocomposites established that the interactions between polymer (organic phase) and intercalated/exfoliated nano-platelets of clay (inorganic phase) at a molecular level enhances the mechanical, thermal, permeation, optical, chemical and electrical properties as compared to the virgin polymer matrix. The hydrophilic nature of linear chain dipolar poly(ethylene oxide) (PEO) and also of montmorillonite (MMT) clay plays an important role in the development of desired physical and electrical properties of the nanocomposite material by adjusting MMT concentration in the polymer matrix. Besides MMT concentration the pre-treatment of mixing and preparation route of the nanocomposites also govern their physical and electrical properties (Shen *et al* 2003; Hikosaka *et al* 2006).

The nanocomposites comprising of PEO with MMT as filler are extensively synthesized by solution intercalation technique and sometimes also by melt compounding process (Tunney and Detellier 1996; Ogata *et al* 1997; Liao *et al* 2001; Shen *et al* 2002, 2003; Chaiko 2003; Strawhecker and Manias 2003; Chen and Evans 2004; Lin-Gibson *et al* 2004; Nelson and Cosgrove 2004; Homminga *et al* 2005; Reinholdt *et al* 2005; Elmahdy *et al* 2006; Hikosaka *et al* 2006; de Bruyn *et al* 2008; Liu *et al* 2008; Miwa *et al* 2008; Sengwa *et al* 2009a; Sengwa and Choudhary 2011). The characterization of these PCNs by various spectroscopic and morphological measurements established that PEO molecules have excellent intercalation in Na^+–MMT and NH_4^+–MMT galleries due to their hydrophilic behaviour, good adhesion and favourable interactions compatibility between the PEO and MMT nano-platelets. Further, the amount of intercalated PEO in MMT galleries and adsorbed PEO on MMT exfoliated surfaces anomalously vary with the increase of MMT concentration (Tunney and Detellier 1996; Ogata *et al* 1997; Liao *et al* 2001; Shen *et al* 2002, 2003; Chaiko 2003; Strawhecker and Manias 2003; Chen and Evans 2004; Lin-Gibson *et al* 2004; Nelson and Cosgrove 2004; Homminga *et al* 2005; Reinholdt *et al* 2005; Elmahdy *et al* 2006; Hikosaka *et al* 2006; de Bruyn *et al* 2008; Liu *et al* 2008; Miwa *et al* 2008; Sengwa *et al* 2010a; Sengwa and Choudhary 2011). As compared to Na^+–MMT, the ion exchange MMT (replacing the original small cations by more bulky one) have large compatibility of polymers to easily intercalate because the bulky ion surface modification increases the MMT interlayer spacing (Passaglia *et al* 2008).

Several investigations on solid and colloidal PCNs confirmed the potential use of dielectric spectroscopy for the structural characterization of dispersed MMT in polymer matrix and the hindrance to polymer chain dynamics

*Author for correspondence (rjsengwa@rediffmail.com)

(Kanapitsas *et al* 2002; Böhning *et al* 2005; Bur *et al* 2005; Noda *et al* 2005; Elmahdy *et al* 2006; Mijović *et al* 2006; Pluta *et al* 2007; Psarras *et al* 2007; Rao and Pochan 2007; Fritzsche *et al* 2008; Kosmidou *et al* 2008; Passaglia *et al* 2008; Sengwa *et al* 2008, 2009a–c, 2010a, b; Wang *et al* 2008; Pandis *et al* 2009; Sengwa and Choudhary 2010, 2011). In addition, the characterization of dielectric properties of PCNs has attracted a lot of attention from on-line process monitoring and off-line measurements (Bur *et al* 2005; Noda *et al* 2005). Further, the synthesization of PCNs of low dielectric constant and loss has large applications in integrated circuits, microelectronic and insulating devices, and membrane technology (Treichel *et al* 1998; Tanaka *et al* 2004). The flexible and linear chain structure of PEO makes large ionic conduction of alkali salt mixed PEO–MMT nanocomposites with improved mechanical and thermal properties for their use as a novel solid electrolyte material for rechargeable batteries at ambient temperature, which is also established by the dielectric/impedance spectroscopic measurements (Chen and Chang 2001; Chen *et al* 2001, 2002; Sandí *et al* 2003; Loyens *et al* 2005; Thakur *et al* 2006; Kim *et al* 2008; Pradhan *et al* 2008; Mohapatra *et al* 2009; Sengwa *et al* 2010c; Choudhary and Sengwa 2011a–c).

In the present paper, an attempt is made to characterize the dielectric behaviour and alternating current (a.c.) electrical conductivity of melt compounded hot-pressed nanocomposites consisting of PEO filled with organophilic montmorillonite (OMMT) clay. In order to confirm the effect of electrode polarization phenomena and bulk material properties, the impedance spectroscopy and electric modulus spectra were also investigated. The dielectric properties were used to confirm the extent of OMMT intercalation and exfoliation in PEO matrix and their effect on polymer chain dynamics. Further the synthesization of PEO–OMMT by melt compounding process is a rapid, least expensive and dry procedure, and the dielectric characterization can provide an idea for their direct use in the fabrication of microelectronic devices and membranes.

2. Materials and methods

2.1 *Materials*

PEO powder of molecular weight 600,000 g/mol and organophilic montmorillonite (OMMT) clay surface modified with 25–30 wt.% trimethyl stearyl ammonium (Nanocor® 1·28 E) were purchased from Sigma-Aldrich, USA.

2.2 *Preparation of nanocomposite films*

For the preparation of PEO–OMMT films, firstly, the required amounts of PEO (3·00, 2·97, 2·94, 2·91, 2·85, 2·70 and 2·40 g) and OMMT (0·00, 0·03, 0·06, 0·09, 0·15, 0·30 and 0·60 g) of 3 g total weight for the OMMT weight fractions (wt%) (0, 1, 2, 3, 5, 10 and 20, respectively) were mechanically mixed using an agate mortar and pestle. After that each PEO–OMMT composition was melt compounded at 70 °C, slightly higher than that of the melting temperature of PEO, 65 °C under 3 tons of pressure in 60 mm diameter stainless steel die with 1 mm spacer using hot-press polymer film making unit and thus melt intercalated PEO–$x$wt% OMMT nanocomposite films of 1 mm thickness were obtained.

2.3 *Measurements*

Agilent 4284A precision LCR meter and Agilent 16451B solid dielectric test fixture were used for the dielectric measurements in the frequency range from 20 Hz to 1 MHz. Frequency dependent values of parallel capacitance, C_P, parallel resistance, R_p and loss tangent, tanδ (dissipation factor, D), of the dielectric test fixture filled with nanocomposite film were measured for the determination of dielectric/electrical spectra of the PEO–$x$wt% OMMT films at 30 °C. Prior to sample measurements, the open circuit calibration was performed to eliminate the effect of stray capacitance of the dielectric test fixture (Agilent Technologies Ltd, Japan 2000). The evaluation of intensive quantities, viz. complex dielectric function, $\varepsilon^*(\omega) = \varepsilon' - j\,\varepsilon''$, alternating current (a.c.), electrical conductivity, $\sigma^*(\omega) = \sigma' + j\,\sigma''$ and, electric modulus, $M^*(\omega) = M' + j\,M''$ and the extensive quantity i.e. complex impedance, $Z^*(\omega) = Z' - j\,Z''$ of the PCNs films are described in detail elsewhere (Sengwa *et al* 2010c; Sengwa and Choudhary 2011).

3. Results and discussion

3.1 *Complex dielectric function and electric modulus spectra*

Figure 1 shows that the real part of complex dielectric function ε' of pure PEO and PEO–OMMT melt compounded films initially decrease with increase of frequency and approaches a constant value at 1 MHz, which corresponds to their static permittivity, ε_s. Inset of figure 1 shows that the ε_s values of these nanocomposites vary anomalously with increase of OMMT concentration. The change in ε' or ε_s values of the PCNs has strong correlation with the predominance of intercalated and exfoliated structural properties of the dispersed clay in the polymer matrix (Kanapitsas *et al* 2002; Wang *et al* 2004a, b; Böhning *et al* 2005; Bur *et al* 2005; Noda *et al* 2005; Elmahdy *et al* 2006; Mijović *et al* 2006; Pluta *et al* 2007; Psarras *et al* 2007; Rao and Pochan 2007; Fritzsche *et al* 2008; Kosmidou *et al* 2008; Passaglia *et al* 2008; Sengwa *et al* 2008, 2009a–c, 2010a, b; Wang *et al* 2008; Pandis *et al* 2009; Sengwa and Choudhary 2010, 2011). It is well established that predominance of MMT exfoliation in the polymer matrix decreases the ε' value whereas intercalation increases it (Wang *et al* 2004a, b; Bur *et al* 2005; Noda *et al* 2005; Sengwa and Choudhary 2010, 2011; Sengwa *et al* 2010b, c). Due to hydrophilic behaviour,

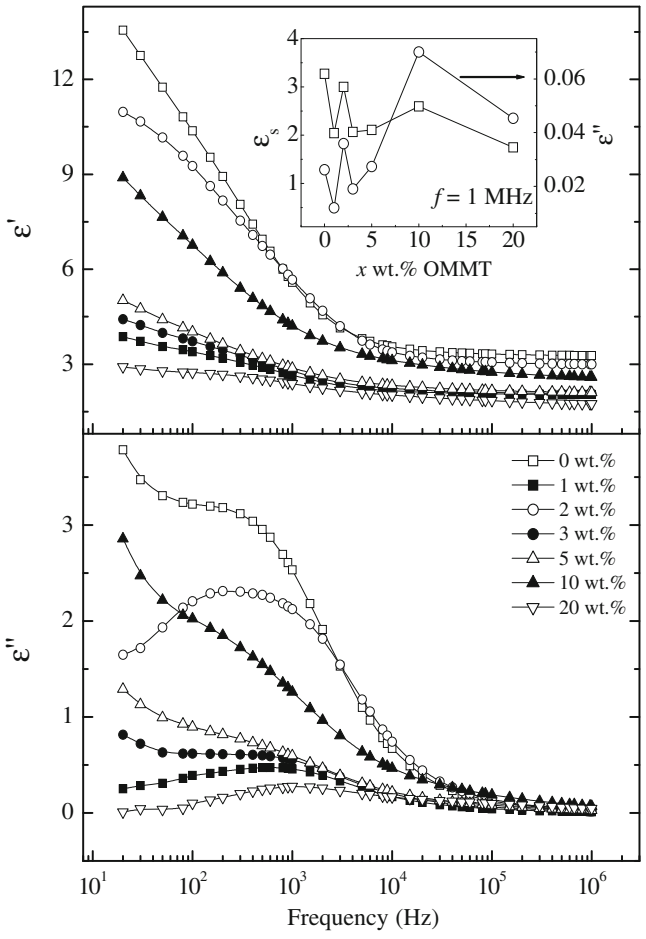

Figure 1. Frequency dependent real part, ε' and loss, ε'', of dielectric function of melt compounded PEO–x wt% OMMT nanocomposite films at 30 °C. Inset shows variation of static permittivity, ε'_s (ε' values) and loss ε'' at 1 MHz against $x$wt% OMMT.

PEO promotes the intercalation of its molecules in Na^+–MMT galleries and also have large adsorption on exfoliated nano-platelets surfaces (Shen *et al* 2002, 2003). After several attempts, the conformation of the intercalated PEO in MMT galleries is still controversial, which is mainly owing to the variation in the mixing process of clay in the PEO matrix, the type of clay used and the route of nanocomposite preparation (Homminga *et al* 2005; Hikosaka *et al* 2006). Further, on comparison with Na^+–MMT, the NH_4^+–MMT surfaces have strong interaction with the adsorbed PEO chains, which also influences MMT structures in PEO matrix (Aranda and Ruiz-Hitzky 1999; Liu 2007).

In the present study, a large decrease in ε_s value with a loading of 1 wt% OMMT (inset of figure 1) confirms that OMMT exfoliation dominates over its intercalated structures. It seems that at 1 wt% OMMT, PEO chains cover more and more OMMT surfaces by adsorption and form the PEO–OMMT micro-aggregates. At 2 wt% OMMT, the ε_s value is close to that of virgin PEO film, which confirms the existence of an equal amount of intercalated and exfoliated OMMT structures. The ε_s values at 3, 5 and 20 wt% OMMT are found nearly equal to that of 1 wt% in PEO matrix, which inferred that OMMT exfoliated structures dominates at these concentrations, but their amount varies anomalously at these OMMT concentrations. Further, the low ε_s value of the nanocomposites as compared to pure PEO film reveals the decrease of crystalline amount of PEO when OMMT is used as filler. Further, at 1 MHz, the ε_s values of PEO–OMMT films are in the range of 2–3 and the dielectric loss ε'' values are <0·07 (inset of figure 1), which suggests their applications as low dielectric constant materials at radio frequencies. These ε_s values of PEO–OMMT films are found to be in agreement with the aqueous solution cast PEO–MMT nanocomposite films (Sengwa and Choudhary 2011).

The ε'' spectra of PEO–OMMT films show the loss peak around 1 kHz, which is corresponding to dielectric relaxation of PEO segmental dynamics (local chain motion), and ε'' values are very small at high frequencies (figure 1). The ε'' peak are not sharp for some of the nanocomposite films, which may be either due to the contribution of ohmic conductivity or the Maxwell–Wagner interfacial polarization that occurs at the interfacing boundaries of different conductivity components in the composite material (Kremer and Schönhals 2003; Sengwa and Choudhary 2011). Due to independence of ε' from ohmic conductivity, the derivative of ε' denoted as $\varepsilon''_{\text{deriv}}$ (Fritzsche *et al* 2008) is used in order to confirm the contribution of conductivity effect in loss spectra, which is derived from the relation:

$$\varepsilon''_{\text{deriv}} = -\frac{\pi}{2}\frac{\partial \varepsilon'(\omega)}{\partial \ln(\omega)} \approx \varepsilon''. \tag{1}$$

Figure 2 shows comparative spectra of ε'' and $\varepsilon''_{\text{deriv}}$ of PEO–1 wt% OMMT film. The inset of figure 2 also includes these spectra for pure PEO film. It is found that (1) is almost exact for these materials and the $\varepsilon''_{\text{deriv}}$ reproduces the measured frequency dependent ε'' data with sharp relaxation peak. Similar behaviour is also observed for various OMMT concentrations of these nanocomposite films. The values of PEO segmental relaxation time, τ_ε, in these nanocomposites were evaluated from the loss peak frequency, $f_p(\varepsilon'')$ in the $\varepsilon''_{\text{deriv}}$ spectra, using the relation (Sengwa *et al* 2010b; Sengwa and Choudhary 2010, 2011):

$$\tau_\varepsilon = (2\pi\, f_p(\varepsilon''))^{-1}. \tag{2}$$

The significant upturn in ε' spectra at lower end side of the PEO–OMMT nanocomposites (figure 1) may be due to the contribution of electrode polarization (EP) effect or the Maxwell Wagner (MW) interfacial polarization process (Sengwa *et al* 2010b; Sengwa and Choudhary 2010, 2011). To confirm this EP effect, electric modulus spectra of the PEO–OMMT nanocomposites (figure 3) were analysed, which is a common practice used in solid dielectric materials (Thakur *et al* 2006; Kosmidou *et al* 2008; Pradhan *et al* 2008; Sengwa *et al* 2008, 2009c, 2010b; Sengwa and Choudhary 2010, 2011). The non-zero values of M' at lower

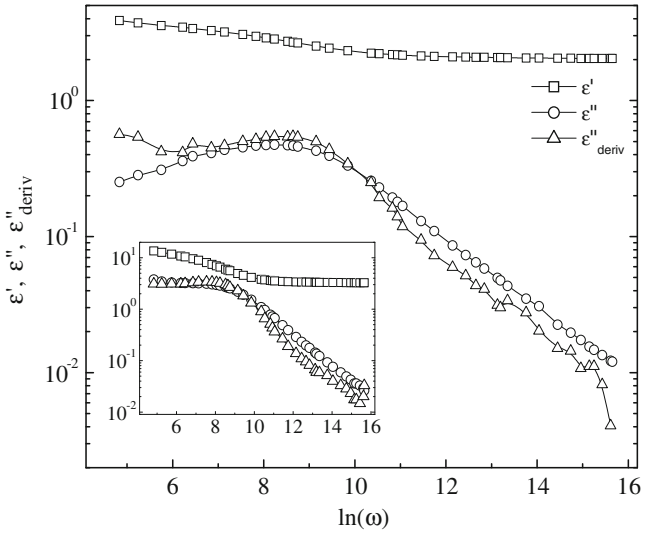

Figure 2. Comparative spectra of real part, ε', loss ε'' and $\varepsilon''_{\text{deriv}}$ of dielectric function of melt compounded PEO–1 wt% OMMT nanocomposite film at 30 °C. Inset shows spectra for pure PEO film.

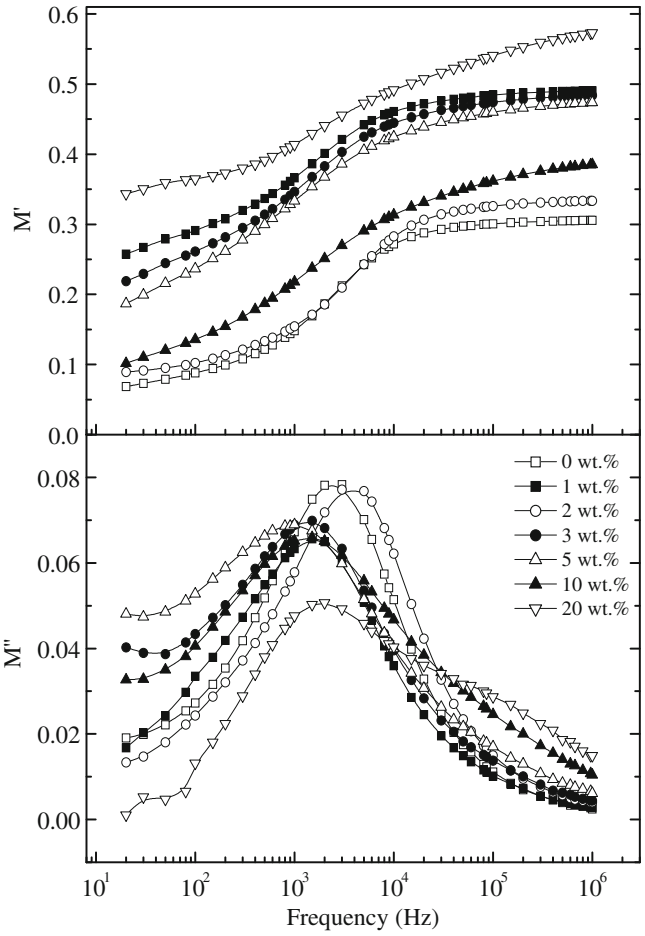

Figure 3. Frequency dependent real part, M' and loss, M'', of electric modulus of melt compounded PEO–$x$wt% OMMT nanocomposite films at 30 °C.

frequency end of the spectra suggest that the electrode polarization relaxation frequency for these materials is beyond the lower limit of experimental frequency range. Sharp peaks in M'' spectra can be attributed to the electric modulus or ionic conduction relaxation (Pradhan *et al* 2008; Choudhary and Sengwa 2011a–c), which are governed by the PEO segmental dynamics. The electric modulus relaxation time, τ_{M}, is determined from the frequency $f_{\text{p}}(M'')$ corresponding to the modulus spectra peak using the relation (Sengwa and Choudhary 2010, 2011):

$$\tau_{\text{M}} = (2\pi f_{\text{p}}(M''))^{-1}. \tag{3}$$

3.2 *A.C. conductivity*

Figure 4 shows that the real part, σ', of a.c. conductivity of pure PEO and PEO–OMMT films increases by 3 orders of magnitude with an increase of alternating field frequency from 20 Hz to 1 MHz. Due to semicrystalline structures of PEO, the $\sigma'(f)$ plots have straight lines of two different slopes, which are distinguished around the tanδ peak frequencies. From figure 4, it can be seen that the lower frequency, $\sigma'(f)$, straight line have higher value of slope as compared to their higher frequency. The $\sigma'(f)$ values of PEO are found to be in good agreement with the earlier reported data at same temperature (Mishra and Rao 1998; Choudhary and Sengwa 2011a–c). The d.c. conductivity, σ_{dc}, of these materials were estimated from the straight line fit of low frequency σ' spectra, and the same are plotted against OMMT concentration in the inset of figure 4. It is observed that up to 10 wt% OMMT loading in PEO matrix, the σ_{dc} values of these nanocomposites vary anomalously within one order of magnitude, but at 20 wt% OMMT there is a decrease in the value of about three orders of magnitude. Further these σ_{dc} values of PEO–OMMT are found about one order of magnitude lower than that of aqueous solution cast PEO–MMT films (Sengwa and Choudhary 2011), which reveals that the mobility of bulky cation of OMMT is less as compared to that of the small cation (Na^+) of MMT.

3.3 *Dielectric relaxation behaviour*

In figure 5, we have plotted the comparative spectra of ε'', M'', tanδ and σ' values of PEO–1 wt.% OMMT nanocomposite as a representative plot. It is found that the tanδ peak frequency for the nanocomposites lies between ε'' and M'' peak frequencies, which is the general characteristic of PCN materials (Sengwa *et al* 2010b; Sengwa and Choudhary 2010, 2011). From figure 5, it is also observed that the transitions in the slopes of σ' spectra occurs at frequency, $f_{\text{p}}(M'')$.

Inset of figure 5 shows that τ_ε and τ_{M} values of the PEO–OMMT nanocomposites vary anomalously with increase in OMMT concentration. These values confirm that the PEO chain segmental motion and the ion conduction mechanism

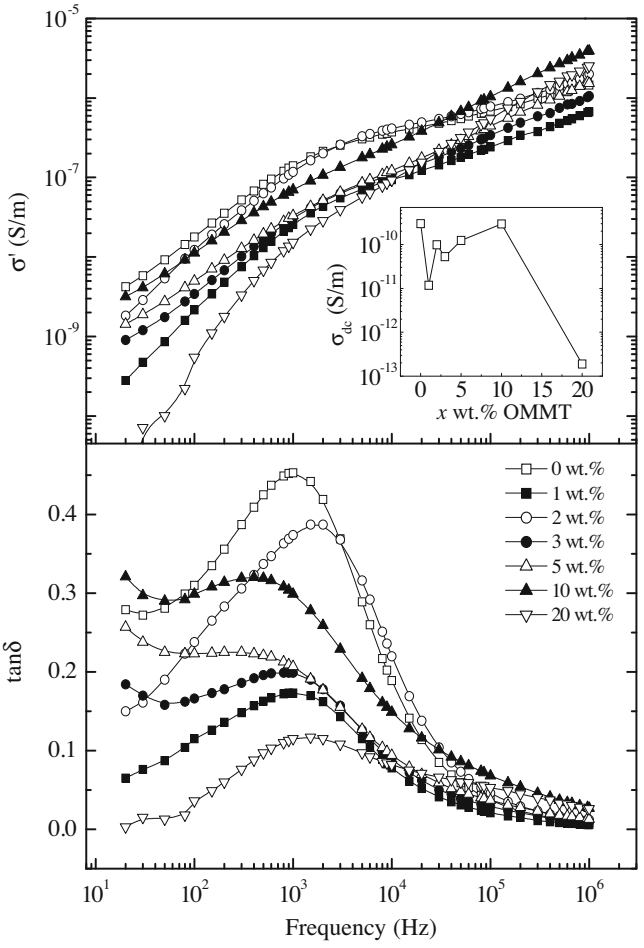

Figure 4. Frequency dependent real part of a.c. conductivity, σ' and loss tangent, tanδ, of the melt compounded PEO–x wt.% OMMT nanocomposite films at 30 °C. Inset shows variation of σ_{dc} with x wt% OMMT.

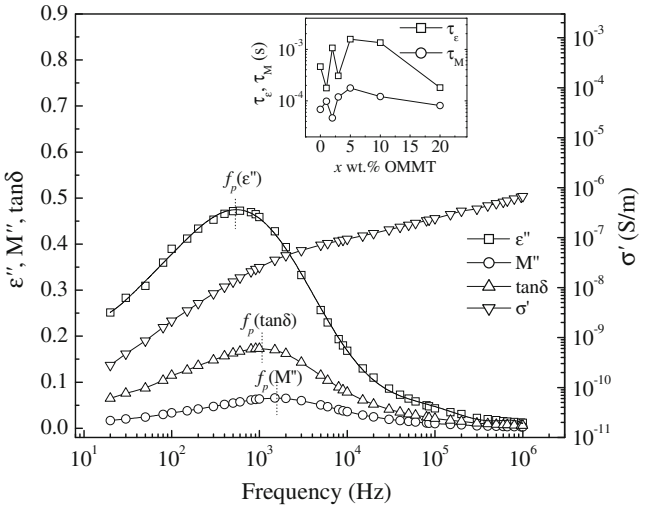

Figure 5. Comparison of ε'', M'', tanδ and σ' spectra of melt compounded PEO–1 wt.% OMMT nanocomposite film at 30 °C. Inset shows variation of τ_ε and τ_M with x wt% OMMT.

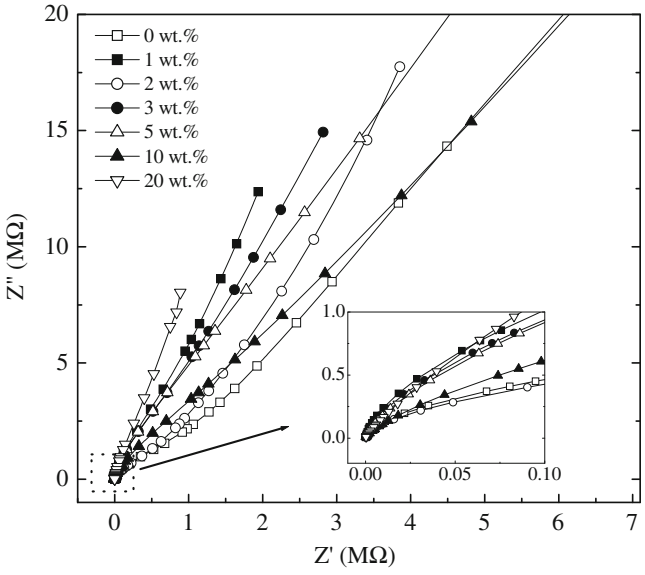

Figure 6. Complex impedance plane plots (Z'' vs Z') of melt compounded PEO–x wt% OMMT nanocomposite films at 30 °C. Inset shows enlarged view at high frequencies.

are affected by the exfoliated and intercalated OMMT structures. The maximum in relaxation times at 5 wt% OMMT confirm the large hindrance to the PEO segmental dynamics and also the ionic motion. The $\tau_M < \tau_\varepsilon$ revealed that the ionic motion is faster than that of the PEO chain segmental motion in the correlated structure of the nanocomposites. Further, the relaxation times of melt compounded PEO–OMMT films were found comparatively higher than that of the solution cast PEO–MMT films (Sengwa and Choudhary 2011), which revealed that the presence of organo ammonium salt on the OMMT nano-platelets surfaces form stronger interactions with ether oxygen of the PEO chain. The enhanced interactions produce large hindrance to the PEO chain segmental dynamics, which results in a comparatively higher relaxation times of PEO–OMMT films.

3.4 *Impedance spectra*

Figure 6 shows that the complex impedance plane plots (Z'' vs Z') of the pure PEO and PEO–OMMT nanocomposites start from the origin and incline at different angles to the real axis. The shape of impedance spectra of a material gives information regarding the electrode polarization (formation of electric double layer between the electrodes and the dielectric material interfaces) and about the current carriers whether they are electrons or ions (Thakur *et al* 2006; Pradhan *et al* 2008; Sengwa *et al* 2008, 2009b, c; Choudhary and Sengwa 2011a–c). Generally ion conducting materials show two different arcs corresponding to electrode polarization in lower frequency region and bulk material properties in upper frequency region (Sengwa *et al* 2010c; Choudhary and Sengwa 2011a–c). For the PEO–OMMT

nanocomposites, single arcs represent the bulk material property, which implies that the charge transfer between the material and the electrodes is not influenced by the electric double layer (EP effect). The appearance of single arcs in complex impedance plane plots also suggests a good electrical contact between the PEO–OMMT films and the nickel-plated cobalt electrodes. These plots suggest that the significant increase in ε' at low frequencies may be mainly due to Maxwell–Wagner interfacial polarization. The large values of Z'' as compared to the Z' confirm a high capacitive behaviour of these nanocomposite films, which is owing to their low value of d.c. conductivity.

4. Conclusions

Here we present detailed structural analysis of PEO–OMMT nanocomposites using various formalisms of dielectric processes. The significant decrease of ε_s at 1 wt% OMMT loading is the evidence of predominance of exfoliated OMMT structures in PEO matrix, whereas at 2 wt% OMMT the ε_s value equal to that of pure PEO film confirms the nearly equal amount of OMMT exfoliated and intercalated structures. The dielectric study revealed that the ε_s value at radio frequencies can be tuned by loading 1 to 2 wt% OMMT in the PEO matrix and synthesization by melt compounding technique for their use as low dielectric constant nanocomposite materials in microelectronic technology. The d.c. conductivity of these PEO based films vary within one order of magnitude with OMMT loading up to 10 wt%. The dielectric and electric modulus relaxation times confirm that in the correlated structures of nanocomposites, the a.c. ionic conduction relaxation is faster than that of the PEO chain segmental dynamics. The hindrance to the PEO segmental motion due to ion-dipolar interactions with OMMT is stronger than that of the PEO interaction with Na^+–MMT.

Acknowledgements

Authors are grateful to the Department of Science and Technology, New Delhi, for providing experimental facilities through project No. SR/S2/CMP-09/2002. One of the authors (SC) is thankful to the University Grants Commission, New Delhi, for the award of a Research Fellowship in Science for Meritorious Students (RFSMS).

References

Agilent 2000 Solid test fixture—Operation and service manual (Japan: Agilent Technologies Ltd) 16451B

Aranda P and Ruiz-Hitzky E 1999 *Appl. Clay Sci.* **15** 119

Böhning M, Goering H, Fritz A, Brzezinka K W, Turky G, Schönhals A and Schartel B 2005 *Macromolecules* **38** 2764

Bur A J, Lee Y H, Roth S C and Start P R 2005 *Polymer* **46** 10908

Chaiko D J 2003 *Chem. Mater.* **15** 1105

Chen B and Evans J R G 2004 *J. Phys. Chem.* **B108** 14986

Chen H W and Chang F C 2001 *Polymer* **42** 9763

Chen H W, Chiu C Y, Wu H D, Shen I W and Chang F C 2002 *Polymer* **43** 5011

Chen W, Xu Q and Yuan R Z 2001 *Compos. Sci. Technol.* **61** 935

Choudhary S and Sengwa R J 2011a *Ionics* (DOI: 10.1007/s11581-011-0585-8)

Choudhary S and Sengwa R J 2011b *Indian J. Pure Appl. Phys.* **49** 204

Choudhary S and Sengwa R J 2011c *Indian J. Eng. Mater. Sci.* **18** 147

de Bruyn J R, Pignon F, Tsabet E and Magnin A 2008 *Rheological Acta* **47** 63

Elmahdy M M, Chrissopoulou K, Afratis A, Floudas G and Anastasiadis S H 2006 *Macromolecules* **39** 5170

Fritzsche J, Das A, Jurk R, Stöckelhuber K W, Heinrich G and Klüppel M 2008 *Express Polym. Lett.* **2** 373

Hikosaka M Y, Pulcinelli S H, Santilli C V, Dahmouche K and Craievich A F 2006 *J. Non-Cryst. Solids* **352** 3705

Homminga D, Goderis B, Dolbnya I, Reynaers H and Groeninckx G 2005 *Polymer* **46** 11359

Kanapitsas A, Pissis P and Kotsilkova R 2002 *J. Non-Cryst. Solids* **305** 204

Kim S, Hwang E J, Jung Y, Han M and Park S J 2008 *Colloid Surface* **A313–314** 216

Kosmidou T V, Vatalis A S, Delides C G, Logakis E, Pissis P and Papanicolaou G C 2008 *Express Polym. Lett.* **2** 364

Kremer F and Schönhals A 2003 *Broadband dielectric spectroscopy* (New York: Springer-Verlag)

Liao B, Song M, Liang H and Pang Y 2001 *Polymer* **42** 10007

Lin-Gibson S, Kim H, Schmidt G, Han C C and Hobbie E K 2004 *J. Colloid Interf. Sci.* **274** 515

Liu P 2007 *Appl. Clay Sci.* **38** 64

Liu T, Chen B and Evans J R G 2008 *Bioinsp. Biomim.* **3** 016005

Loyens W, Maurer F H J and Jannasch P 2005 *Polymer* **46** 7334

Mijović J, Lee H, Kenny J and Mays J 2006 *Macromolecules* **39** 2172

Mishra R and Rao K J 1998 *Solid State Ionics* **106** 113

Miwa Y, Drews A R and Schlick S 2008 *Macromolecules* **41** 4701

Mohapatra S R, Thakur A K and Choudhary R N P 2009 *J. Power Sources* **191** 601

Nelson A and Cosgrove T 2004 *Langmuir* **20** 2298, 10382

Noda N, Lee Y H, Bur A J, Prabhu V M, Snyder C R, Roth S C and McBrearty M 2005 *Polymer* **46** 7201

Ogata N, Kawakage S and Ogihara T 1997 *Polymer* **38** 5115

Pandis C *et al* 2009 *J. Polym. Sci.: Part B: Polym. Phys.* **47** 407

Passaglia E, Bertoldo M, Ciardelli F, Prevosto D and Lucchesi M 2008 *Eur. Polym. J.* **44** 1296

Pluta M, Jeszka J K and Boiteux G 2007 *Eur. Polym. J.* **43** 2819

Pradhan D K, Choudhary R N P and Samantaray B K 2008 *Express Polym. Lett.* **2** 630

Psarras G C, Gatos K G, Karahaliou P K, Georga S N, Krontiras C A and Karger-Kocsis J 2007 *Express Polym. Lett.* **1** 837

Rao Y and Pochan J M 2007 *Macromolecules* **40** 290

Reinholdt M X, Kirkpatrick R J and Pinnavaia T J 2005 *J. Phys. Chem.* **B109** 16296

Sandí G, Carrado K A, Joachin H, Lu W and Prakash J 2003 *J. Power Sources* **119–121** 492

Sengwa R J and Choudhary S 2010 *Express Polym. Lett.* **4** 559

Sengwa R J and Choudhary S 2011 *J. Macromol. Sci. Part B: Phys.* **50** 1313

Sengwa R J, Choudhary S and Sankhla S 2008 *Express Polym. Lett.* **2** 800

Sengwa R J, Choudhary S and Sankhla S 2009a *Colloid Surface* **A336** 79
Sengwa R J, Choudhary S and Sankhla S 2009b *Polym. Int.* **58** 781
Sengwa R J, Sankhla S and Choudhary S 2009c *Colloid Polym. Sci.* **287** 1013
Sengwa R J, Choudhary S and Sankhla S 2009d *Indian J. Eng. Mater. Sci.* **16** 395
Sengwa R J, Sankhla S and Choudhary S 2010a *Indian J. Pure Appl. Phys.* **48** 196
Sengwa R J, Choudhary S and Sankhla S 2010b *Compos. Sci. Technol.* **70** 1621
Sengwa R J, Sankhla S and Choudhary S 2010c *Ionics* **16** 697
Shen Z, Simon G P and Cheng Y B 2002 *Polymer* **43** 4251
Shen Z, Simon G P and Cheng Y B 2003 *Eur. Polym. J.* **39** 1917
Strawhecker K E and Manias E 2003 *Chem. Mater.* **15** 844
Tanaka T, Montanari G C and Mülhaupt R 2004 *IEEE Trans. Dielect. Elect. Insul.* **11** 763
Thakur A K, Pradhan D K, Samantaray B K and Choudhary R N P 2006 *J. Power Sources* **159** 272
Treichel H, Ruhl G, Ansmann P, Würl R, Müller Ch and Dietimeier M 1998 *Microelect. Eng.* **40** 1
Tunney J J and Detellier C 1996 *Chem. Mater.* **8** 927
Wang H W, Chang K C, Yeh J M and Liou S J 2004a *J. Appl. Polym. Sci.* **91** 1368
Wang H W, Chang K C, Chu H C, Liou S J and Yeh J M 2004b *J. Appl. Polym. Sci.* **92** 2402
Wang J H, Liang G Z, Yan H X and He S B 2008 *Express Polym. Lett.* **2** 118